

Inhibition of the Class C β -Lactamase from *Acinetobacter* spp.: Insights into Effective Inhibitor Design[†]

Sarah M. Drawz,[‡] Maja Babic,[@] Christopher R. Bethel,[#] Magda Taracila,[@] Anne M. Distler,^{||,○} Claudia Ori,[∇] Emilia Caselli,[∇] Fabio Prati,^{*,∇} and Robert A. Bonomo^{*,#,§,||,⊥}

[‡]Departments of Pathology, [§]Medicine, ^{||}Pharmacology, [⊥]Molecular Biology and Microbiology, Case Western Reserve University School of Medicine, Cleveland, Ohio 44106, [@]Division of Infectious Disease and HIV Medicine, University Hospitals Case Medical Center, and [#]Research Service, Louis Stokes Cleveland Department of Veterans Affairs Medical Center, Cleveland, Ohio 44106, and [∇]Department of Chemistry, University of Modena and Reggio Emilia, 41100 Modena, Italy. [○]Current address: Department of Chemistry, Cuyahoga Community College, Highland Hills, Ohio 44122.

Received September 11, 2009; Revised Manuscript Received November 19, 2009

ABSTRACT: The need to develop β -lactamase inhibitors against class C cephalosporinases of Gram-negative pathogens represents an urgent clinical priority. To respond to this challenge, five boronic acid derivatives, including a new cefoperazone analogue, were synthesized and tested against the class C cephalosporinase of *Acinetobacter baumannii* [*Acinetobacter*-derived cephalosporinase (ADC)]. The commercially available carbapenem antibiotics were also assayed. In the boronic acid series, a chiral cephalothin analogue with a *meta*-carboxyphenyl moiety corresponding to the C₃/C₄ carboxylate of β -lactams showed the lowest K_i (11 ± 1 nM). In antimicrobial susceptibility tests, this cephalothin analogue lowered the ceftazidime and cefotaxime minimum inhibitory concentrations (MICs) of *Escherichia coli* DH10B cells carrying *bla*_{ADC} from 16 to 4 μ g/mL and from 8 to 1 μ g/mL, respectively. On the other hand, each carbapenem exhibited a K_i of < 20 μ M, and timed electrospray ionization mass spectrometry (ESI-MS) demonstrated the formation of adducts corresponding to acyl–enzyme intermediates with both intact carbapenem and carbapenem lacking the C₆ hydroxyethyl group. To improve our understanding of the interactions between the β -lactamase and the inhibitors, we constructed models of ADC as an acyl–enzyme intermediate with (i) the *meta*-carboxyphenyl cephalothin analogue and (ii) the carbapenems, imipenem and meropenem. Our first model suggests that this chiral cephalothin analogue adopts a novel conformation in the β -lactamase active site. Further, the addition of the substituent mimicking the cephalosporin dihydrothiazine ring may significantly improve affinity for the ADC β -lactamase. In contrast, the ADC–carbapenem models offer a novel role for the R₂ side group and also suggest that elimination of the C₆ hydroxyethyl group by retroaldolic reaction leads to a significant conformational change in the acyl–enzyme intermediate. Lessons from the diverse mechanisms and structures of the boronic acid derivatives and carbapenems provide insights for the development of new β -lactamase inhibitors against these critical drug resistance targets.

Acinetobacter spp. are Gram-negative pathogens responsible for an increasing number of serious nosocomial infections, including hospital-acquired pneumonia, urinary tract infections,

and bacteremia (1–4). This nonfermentive, aerobic pathogen harbors multiple antibiotic resistance determinants, including chromosomal AmpC β -lactamase enzymes, OXA carbapenemases, metallo- β -lactamases, and multidrug resistance (MDR)¹ efflux pumps (5, 6). In addition, changes in outer membrane proteins decrease the permeability to antimicrobials (7). Besides intrinsic resistance, *Acinetobacter* spp. possess the ability to acquire new resistance determinants through gene mutations, derepression, and transfer from other organisms. These remarkable attributes can lead to infections resistant to all available β -lactam antibiotics (8, 9). Consequently, treatment of patients with *Acinetobacter* spp. infections is very challenging, and therapeutic options are severely limited for MDR strains (10–12).

One strategy for restoring the efficacy of β -lactam antibiotics is the development of novel β -lactamase inhibitors. Boronic acid derivatives are compounds that replace the β -lactam ring with boronic acid. The boron atom forms a reversible, dative covalent bond with the active site serine of class A and C β -lactamases, assuming a geometry that resembles the tetrahedral transition

[†]This work was supported in part by the Department of Veterans Affairs Merit Review Program and National Institutes of Health (NIH) Grant 1R01 A1063517-01. R.A.B. is also supported by the Veterans Integrated Service Network 10 Geriatric Research, Education, and Clinical Center. S.M.D. was supported in part by NIH Grant T32 GM07250 and the Case Western Reserve University (CWRU) Medical Scientist Training Program. M.B. was supported by the Wyeth Fellowship in Antimicrobial Resistance at CWRU. F.P., E.C., and C.O. gratefully thank Fondazione Cassa di Risparmio di Modena for financial support.

*To whom correspondence should be addressed. R.A.B.: phone, (216) 791-3800, ext. 4399; fax, (216) 231-3482; e-mail, robert.bonomo@med.va.gov. F.P.: phone, +39 059 205 5056; fax, +39 059 373 543; e-mail, prati.fabio@unimore.it.

Abbreviations: ADC, *Acinetobacter*-derived cephalosporinase; amu, atomic mass unit; EI MS, electron impact mass spectrometer; ESI-MS, electrospray ionization mass spectrometry; IPTG, isopropyl β -D-thiogalactopyranoside; MIC, minimum inhibitory concentration; MDR, multidrug resistant; NCF, nitrocefin; PBC, periodic boundary conditions; PDB, Protein Data Bank; THF, tetrahydrofuran.

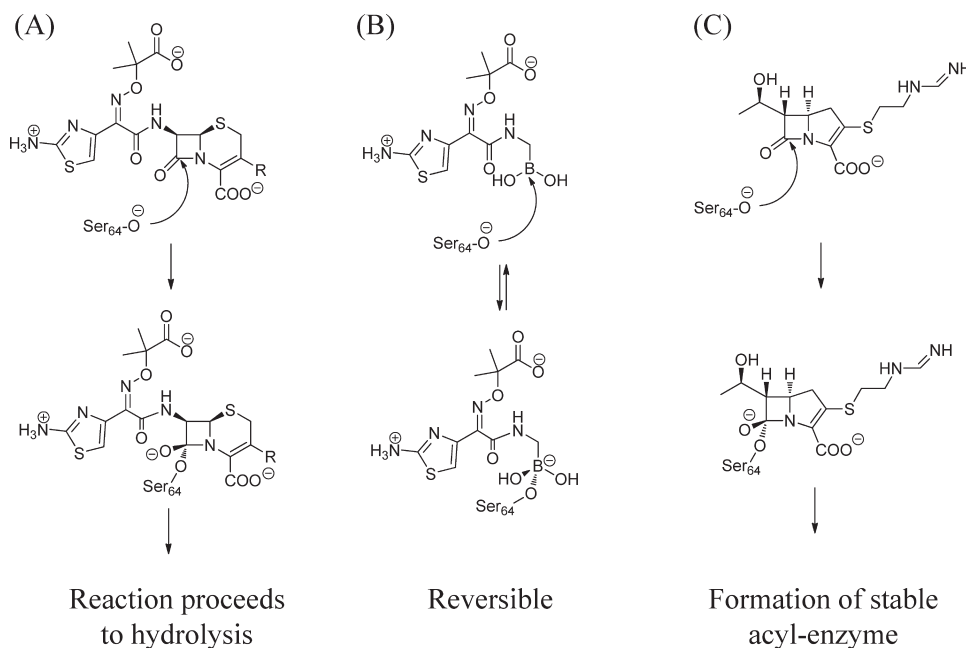


FIGURE 1: Schemes illustrating the interactions of a serine β -lactamase with (A) the cephalosporin ceftazidime, (B) the boronic acid ceftazidime analogue, compound **2**, and (C) the carbapenem imipenem.

state of the β -lactamase hydrolytic reaction (Figure 1) (13, 14). Via modification of the boronic acid substituents to resemble in structure, distance, and stereochemical arrangement the R_1 side chains of natural substrates, affinities in the nanomolar range against class C enzymes of *Escherichia coli* are achieved (15–17).

A second approach to counteracting β -lactamase-mediated antibiotic resistance is the design of β -lactams that resist hydrolysis. Through the combined efforts of natural product screens and medicinal chemistry, β -lactamase-stable penem and cephem derivatives have been modified and synthesized. The most potent β -lactams are the derivatives of thienamycin (i.e., imipenem, meropenem, ertapenem, and doripenem). Carbapenems act as inhibitors of class A, class C, and certain class D β -lactamases by forming a prolonged acyl-enzyme intermediate with the β -lactamase that is very slowly hydrolyzed (18–25).

The *Acinetobacter*-derived cephalosporinases (ADCs) are class C β -lactamases found in *Acinetobacter baumannii* and *Acinetobacter* genomospecies 3 and are responsible for resistance to penicillins, cephalosporins, and β -lactam- β -lactamase inhibitor combinations (26). These AmpC β -lactamases demonstrate a remarkable k_{cat} for first-generation cephalosporins and relatively low affinity for the commercially available β -lactamase inhibitors (26). Therefore, ADC enzymes can serve as important targets for the design of new mechanism-based inactivators. To date, the search for effective inhibitors for the ADC β -lactamase remains challenging. To this end, we synthesized and tested a panel of boronic acid derivatives with specific side chains to serve as chemical probes. We also designed a novel boronate that contained the R_1 side chain of cefoperazone. Concurrently, we explored the role of the R_2 side chain of four different carbapenems in the inhibition of ADC. Taken together, our results indicate that the interactions between the ADC β -lactamase and inhibitors' scaffolds and side chains yield important insights into the properties of class C enzyme active sites.

MATERIALS AND METHODS

Antibiotics and Inhibitors. Ceftazidime and cefotaxime were purchased from Sigma (St. Louis, MO). The chemical structures

of cephalothin and inhibitors studied are shown in Figure 2. The boronic acid ceftazidime analogue and cephalothin analogues were synthesized as previously described (15, 17). The chiral cephalothin analogues **4** and **5** were obtained in the enantiomerically pure form. Imipenem and ertapenem were obtained from Merck & Co. Inc. (Whitehouse Station, NJ). Meropenem was purchased from AstraZeneca Pharmaceuticals (Wilmington, DE) and doripenem from Ortho-McNeil Pharmaceutical Inc. (Raritan, NJ).

Synthesis of the Cefoperazone Analogue. Cefoperazone analogue **1** was synthesized according to the general protocol for the other boronic acid derivatives by acylation of pinacol bis-(trimethylsilyl)aminomethaneboronate with the commercially available cefoperazone acid, promoted by isobutyl chloroformate (17). Triethylamine (231 μL , 1.66 mmol) and isobutyl chloroformate (216 μL , 1.66 mmol) were added to a solution of (2*R*)-2-[(4-ethyl-2,3-dioxopiperaziny)carbonylamino]-2-(4-hydroxyphenyl)acetic acid (530 mg, 1.66 mmol) in anhydrous tetrahydrofuran (THF, 60 mL) at 0 $^{\circ}\text{C}$ and allowed to react under an argon atmosphere for 1 h. A solution of bis-(trimethylsilyl)aminomethaneboronate (500 mg, 1.66 mmol) in anhydrous THF (5 mL), previously treated for 30 min with anhydrous methanol (1.74 mmol), was added at the same temperature. After 20 min, the cooling bath was removed and the mixture was allowed to react overnight at room temperature. Thereafter, the reaction mixture was diluted with diethyl ether (60 mL), and the precipitate (triethylammonium chloride) was removed by filtration. The solvent was distilled under reduced pressure, and the solid residue crystallized from ethyl acetate, affording the title compound as a whitish solid (54% yield); $[\alpha]_{\text{D}} -59.0$ (*c* 0.8, CH_3OH). The pinacol ester spontaneously hydrolyses in the phosphate buffer, generating the corresponding cefoperazone boronic acid.

^1H and ^{13}C NMR spectra of compound **1** were recorded on a Bruker DPX-200 spectrometer. The chemical shifts (δ) are reported in parts per million downfield from the internal standard, tetramethylsilane (s, singlet; d, doublet; t, triplet; q, quartet; m, multiplet). Mass fragmentations were determined on

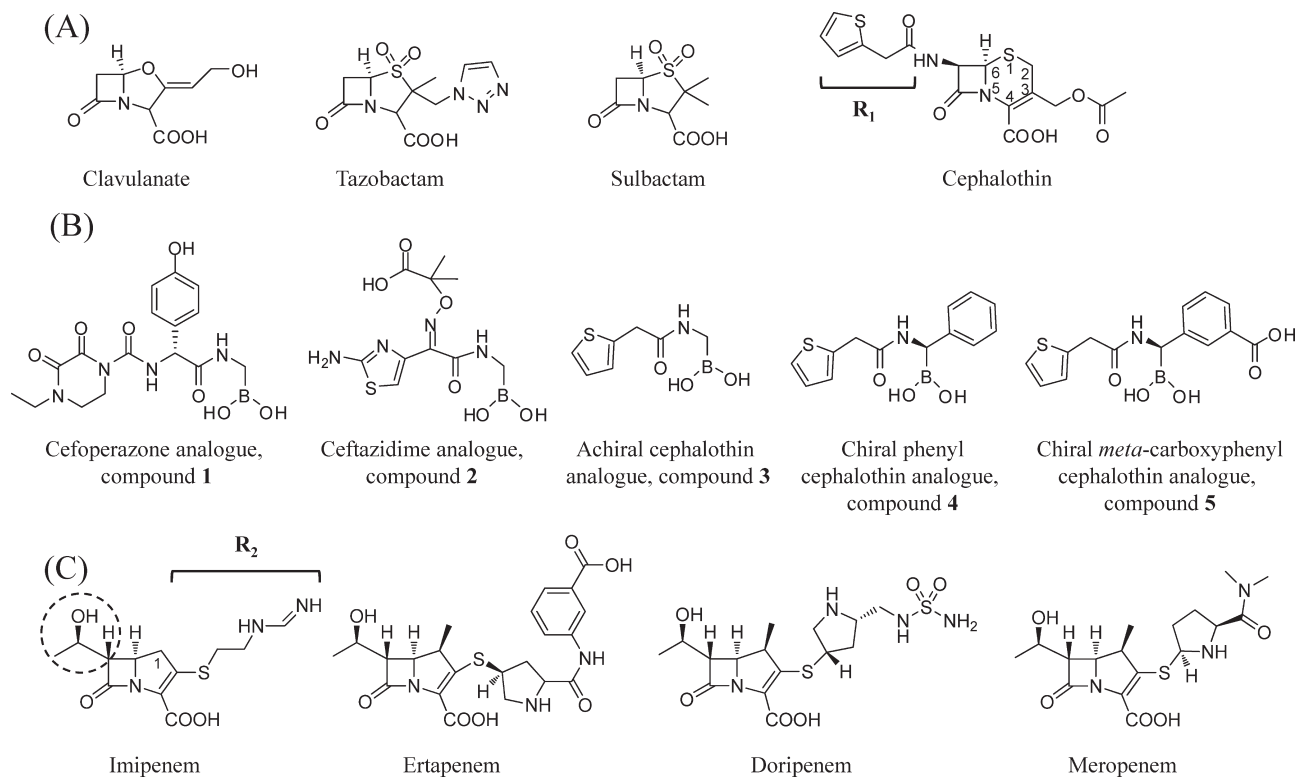


FIGURE 2: Chemical structures of (A) commercially available inhibitors and cephalosporin substrate cephalothin, (B) boronic acid derivatives, and (C) carbapenems used in this study. The cephalothin structure is labeled with the accepted ring numbering system. The C₆ hydroxyethyl group of imipenem, which may be eliminated after formation of the acyl–enzyme intermediate, is circled in dashed lines.

a Finnigan MAT S50 Q electron impact mass spectrometer (EI MS, 70 eV): ¹H NMR (200 MHz, DMSO-*d*₆) δ 1.07 (3H, t, *J* = 7.2 Hz, CH₂CH₃), 1.15 (12H, s, CH₃ pic), 2.44 (2H, d, *J* = 3.7 Hz, NCH₂B), 3.38 (2H, q, *J* = 7.2 Hz, CH₂CH₃), 3.48–3.62 (2H, m, CH₂ pip), 3.82–3.96 (2H, m, CH₂ pip), 5.32 (1H, d, *J* = 7.3 Hz, CHPh), 6.71 (2H, d, *J* = 8.5 Hz, meta), 7.19 (2H, d, *J* = 8.5 Hz, ortho), 8.41 (1H, t, *J* = 3.7 Hz, NH), 9.14 (1H, s, OH), 9.64 (1H, d, *J* = 7.3 Hz, NH); ¹³C NMR (50 MHz, DMSO-*d*₆) δ 12.3, 25.1, 25.2, 40.8, 42.1, 43.3, 56.5, 83.3, 115.5, 128.7, 129.2, 152.3, 155.9, 157.5, 159.8, 170.6; EI MS *m/z* (%) 474 (M⁺, 0.2), 458 (0.4), 400 (2), 374 (2), 332 (14), 317 (10), 275 (16), 274 (96), 273 (36), 216 (19), 173 (9), 148 (18), 142 (58), 121 (35), 120 (46), 99 (100), 83 (15).

Genetic Constructs and Host Strains. For large-scale protein expression and β-lactamase characterization, the *bla*_{ADC} gene (specifically, *bla*_{ADC-7}) was cloned into the pET24a(+) vector (kanamycin resistant, Novagen, Madison, WI) following a previously published method (26). After sequencing verification, the correct construct was maintained in *E. coli* DH10B cells and transformed into *E. coli* BL21(DE3) cells for protein expression. For MIC determinations, *bla*_{ADC} was directionally cloned into the pBC SK(+) phagemid vector (chloramphenicol resistant, Stratagene, La Jolla, CA) as previously described (26). Briefly, the pET24a(+) *bla*_{ADC} construct was digested with XbaI and BamHI in Multi-Core buffer (Promega, Madison, WI), preserving the 5' upstream flanking region from the pET24a(+) vector in front of the insert when ligated into pBC SK(+).

Antimicrobial Susceptibility (MICs). *E. coli* DH10B cells expressing the *bla*_{ADC} gene were phenotypically characterized by lysogeny broth agar dilution MICs. The MICs for various antibiotics were determined using a Steers Replicator that delivered 10 μL of a diluted overnight culture containing 10⁴

colony forming units. The cephalothin analogues 3 and 5 were tested at a constant concentration of 4 μg/mL in combination with either ceftazidime or cefotaxime.

β-Lactamase Purification. The ADC β-lactamase was prepared from *E. coli* BL21(DE3) cells after induction with isopropyl β-D-thiogalactopyranoside (IPTG). Cultures (500 mL) were induced at an optical density at 600 nm of 0.5–0.8 (final IPTG concentration of 0.2 mM) at 37 °C for 4 h in lysogeny broth. These cells were pelleted and resuspended in 50 mM Tris (pH 7.4) and β-lactamase liberated with lysozyme and EDTA per established methods (28). Accordingly, the ADC protein was purified by preparative isoelectric focusing and fast protein liquid chromatography with a Sephadex Hi Load 26/60 column (Pharmacia, Uppsala, Sweden) (29). The enzyme was quantified, purity assessed by sodium dodecyl sulfate–polyacrylamide gel electrophoresis, and size verified by mass spectrometry (26).

Kinetics. Steady state kinetics were performed on an Agilent (Palo Alto, CA) 8453 diode array spectrophotometer. Each continuous assay was performed in 10 mM phosphate-buffered saline (pH 7.4) at room temperature. *K_i* values were calculated by measurement of the initial velocity in the presence of a constant concentration of enzyme (3 nM), and increasing concentrations of the inhibitors (ranging from 50 nM to 500 μM) competed against the indicator substrate nitrocefin (NCF) (BD Biosciences, San Jose, CA) (Δε₄₈₂ = 17400 M⁻¹ cm⁻¹). The *K_i* values were corrected to account for the affinity of NCF for ADC using the following equation (30):

$$K_i(\text{corrected}) = K_i(\text{observed}) / (1 + [S] / K_{m\text{NCF}}) \quad (1)$$

Due to time-dependent inhibition of chiral boronic acid derivatives, compounds 4 and 5 were preincubated with enzyme

for 5 min in phosphate-buffered saline before the reaction was initiated with the addition of substrate, as described previously (15, 27, 31–33). In earlier experiments, preincubation of the achiral compound **3** with enzyme did not affect the K_i determination (data not shown).

Electrospray Ionization Mass Spectrometry (ESI-MS). Mass spectrometry was performed to determine products of inactivation. We incubated 14 μM ADC for 15 min with and without compounds **2** and **5** and each carbapenem at an inhibitor:enzyme ratio of 20:1. Each reaction was terminated by the addition of 0.1% trifluoroacetic acid and each mixture immediately desalted and concentrated using a C₁₈ ZipTip (Millipore, Bedford, MA) according to the manufacturer's protocol. Samples were then placed on ice and analyzed within 1 h.

Spectra of the intact ADC–inhibitor proteins were generated on a Q-STAR XL Quadrupole-Time-of-Flight mass spectrometer (Applied Biosystems, Framingham, MA) equipped with a nanospray source. Experiments were performed by diluting the protein sample with a 50% acetonitrile/0.1% trifluoroacetic acid mixture to a concentration of 10 μM . This protein solution was then infused at a rate of 0.5 $\mu\text{L}/\text{min}$, and the data were collected for 2 min. Spectra were deconvoluted using Analyst (Applied Biosystems). All measurements have an error of ± 3 atomic mass units (amu).

Molecular Representations. The ADC model was generated by the SWISS-MODEL automated protein structure homology modeling server (available at <http://swissmodel.expasy.org>) using the deposited GenBank ADC-7 protein sequence (AY648950) and the *Enterobacter aerogenes* CMY-10 β -lactamase as a template (Protein Data Bank entry 1ZKJ) (34, 35). We optimized the generated model by energy minimization using Discovery Studio version 2.1 (Accelrys, San Diego, CA). The minimization was performed in several steps, using a steepest descent and conjugate gradient algorithm to reach the minimum convergence (0.02 kcal mol⁻¹ Å⁻¹). The protein was immersed in a water box, 7 Å from any face of the box, and the solvation model used was with periodic boundary conditions (PBC). The force field parameters of CHARMM were used for minimization, and the particle mesh Ewald method was used to treat long-range electrostatics. The bonds that involved hydrogen atoms were constrained with the SHAKE algorithm. Following equilibration, two separate 2 fs molecular dynamics simulations (heating–cooling and production) at a constant pressure and temperature (300 K) were conducted for the ADC model. The trajectories were analyzed, and the minimum energy conformation was chosen.

To verify the quality of the ADC β -lactamase model, we used the Protein Structure and Model Assessment Tools available at <http://swissmodel.expasy.org> (see Figures 1–3 of the Supporting Information). The atomic empirical mean force potential (ANOLEA) evaluation of the model's packing quality showed that 98% of the amino acids were in the favorable energy environment (36). We validated the stereochemical quality of the ADC model using Procheck which compares the geometry of protein residues with the stereochemical parameters of well-refined, high-resolution structures (37). Additionally, 97.5% of the non-proline, non-glycine residues in the ADC model were in the most favorable region of a Ramachandran plot.

The Align Multiple Sequences function of Discovery Studio version 2.1 allowed us to compare the generated ADC protein structure with that of the deposited crystal structure coordinates for the *Enterobacter cloacae* P99 enzyme (PDB entry 1XX2) and

Table 1: K_i Values of Inhibitors in Direct Competition Assays with ADC

inhibitor	K_i (μM)
commercially available class A inhibitors	
clavulanate	4275 \pm 253 ^a
sulbactam	109 \pm 3 ^a
tazobactam	91 \pm 21 ^a
boronic acid derivatives	
compound 1	0.60 \pm 0.06
compound 2	0.31 \pm 0.03
compound 3	0.78 \pm 0.02
compound 4	0.036 \pm 0.008
compound 5	0.011 \pm 0.001
carbapenems	
imipenem	1.3 \pm 0.1
ertapenem	5.8 \pm 0.2
doripenem	12.2 \pm 0.4
meropenem	19 \pm 2

^a K_i values obtained previously by the same methodology (26).

E. coli AmpC (PDB entry 2BLS). The program uses a method based on CLUSTAL W which aligns multiple sequences using a progressive pairwise alignment algorithm (38). A multiple-sequence alignment is generated, and secondary structure matches graded as identical, strong, weak, or nonmatching are based on the calculated alignment score.

The minimized and equilibrated ADC model was used for constructing the acylation complexes of the ADC β -lactamase and the chiral cephalothin analogue **5**, imipenem, and meropenem ligands. The ligand structures were built using Discovery Studio Fragment Builder tools. The CHARMM force field was applied; the molecule was solvated with PBC and minimized using a Standard Dynamics Cascade protocol (one minimization using the steepest descent algorithm, followed by the adopted basis Newton–Raphson algorithm and three subsequent dynamics stages at NVT and 300 K).

The minimized ligands were docked in the active site of the enzyme using LibDock (39). The generated conformations (30–40) were manually analyzed and the most favorable ones chosen. The complex between the ligand and the enzyme was created, solvated, and energy-minimized. The acyl–enzyme complex was created by making a bond with Ser64, and the assembly was further minimized using the conjugate gradient algorithm with PBC to 0.001 minimum derivative. To reach the minimum equilibrium, the complexes were equilibrated using molecular dynamics simulations.

RESULTS

Kinetics. Table 1 summarizes our kinetic analysis of the inhibition of ADC β -lactamase. To establish a comparison, we list the previously reported K_i values of the commercially available β -lactamase inhibitors against ADC; these K_i values are not in the range that would translate into effective inhibition in MIC testing (26).

In contrast, we found that the boronic acid derivatives containing the R₁ side chain of cephalosporins bind the class C ADC with K_i values in the nanomolar range. The cefoperazone analogue and the ceftazidime analogue, compounds **1** and **2**, respectively, exhibit K_i values of ≤ 1 μM . Compound **5** with the cephalothin R₁ side chain and the *meta*-carboxyphenyl ring, which has a carboxylate that is designed to mimic the geometry and distances of the conserved C₄ carboxylate of cephalosporin

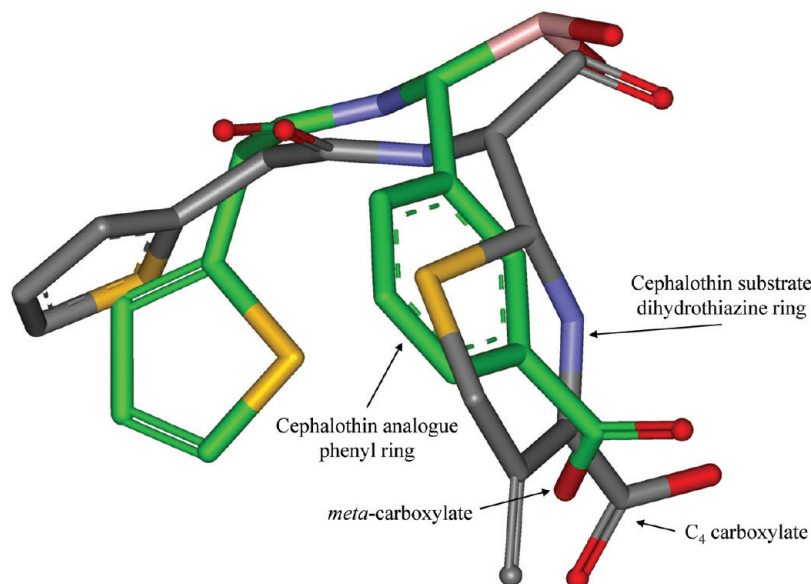


FIGURE 3: Overlay of the molecular coordinates for the *E. coli* AmpC covalently bound to the cephalothin substrate (colored by atom, PDB entry 1KVM) and boronic acid chiral cephalothin analogue, compound **5** (colored green, PDB entry 1MXO). The position of cephalothin's dihydrothiazine ring and C₄ carboxylate is shown relative to the *meta*-carboxyphenyl group of compound **5**, which is designed to mimic its stereochemistry and geometry the conserved β -lactam carboxylate.

β -lactams (Figure 3), had the lowest K_i for ADC (11 ± 1 nM). We interpret the 70-fold difference in K_i values between compounds **3** and **5** to mean that the *meta*-carboxyphenyl moiety contributes significantly to the binding of this inhibitor with the ADC β -lactamase. However, compound **4**, which lacks only the *meta*-carboxylate as compared to **5**, also had a low K_i of 36 ± 8 nM.

Because inhibition reactions with the boronic acid derivatives are reversible, we quantified the binding energy contribution of these substituents by using K_i as an equilibrium constant in the Gibbs free energy equation (15):

$$\Delta\Delta G = -RT \ln[(K_i5)/(K_i3)] \quad (2a)$$

Compared to the achiral cephalothin analogue **3**, we determined that the *meta*-carboxyphenyl group on the chiral cephalothin analogue **5** contributes 2.5 kcal/mol in binding energy to ADC. The presence of the *meta*-carboxylate provides 0.7 kcal/mol of the 2.5 kcal/mol provided by this substituent:

$$\Delta\Delta G = -RT \ln[(K_i5)/(K_i4)] \quad (2b)$$

On the basis of these calculations, we maintain that the presence of the phenyl group, which approximates the cephalosporin's dihydrothiazine ring, is largely responsible for the low K_i values of compounds **4** and **5**.

Carbapenems are highly effective β -lactam antibiotics in the treatment of Gram-negative bacteria. Furthermore, carbapenems form prolonged acyl-enzyme intermediates with class C β -lactamases which can effectively inhibit the enzyme. We chose the four commercially available carbapenems to explore the determinants that contribute to the inactivation of ADC β -lactamase. Carbapenems, as ADC AmpC inhibitors, demonstrated low K_i values (ranging from 1.3 ± 0.1 to 19 ± 2 μ M). Comparing the carbapenems with different R₂ side chains, we see that the least substituted, imipenem, has the lowest K_i . The penem scaffold on which these β -lactams are constructed is similar; thus, we assign the differences in K_i values among these carbapenems to the interactions of the β -lactamase with the R₂ side chain.

Table 2: ESI-MS Analysis (amu) of ADC Alone and Incubated with Inhibitors^a

	predicted molecular weight of β -lactamase or inhibitor	species observed in deconvoluted spectra	Δ difference from the β -lactamase molecular weight
ADC alone	40631	40638	7
ADC with inhibitor			
compound 2	330	40637	1
compound 5	319	40638	0
imipenem	299	40936	298
		40893	255
ertapenem	476	41112	474
		41069	431
doripenem	420	41058	420
		41015	377
meropenem	383	41021	383
		40979	341

^aAll measurements have an error of ± 3 amu.

ESI-MS and the Nature of Inactivation Products. We performed timed ESI-MS with ADC, compounds **2** and **5**, and the carbapenems to detect covalent intermediates in the inactivation pathway. As shown in Table 2 and Figure 4, analysis of the ADC-**2** and ADC-**5** reactions using ESI-MS shows that the β -lactamase is unmodified. This result is expected as boronates undergo reversible inhibition. In contrast, when ADC was reacted with the carbapenems, the predominant mass adduct formed corresponded to the sum of the molecular weights of the enzyme and the inhibitor, suggesting the formation of a non-fragmented covalent acyl-enzyme product. This result is consistent with MS data of the carbapenems forming acyl-enzyme intermediates with the class A SHV-1 β -lactamase (21). In addition, the ESI-MS analysis of each ADC-carbapenem spectrum included a small adduct which was the mass equivalent of the carbapenem and β -lactamase minus 43 ± 3 Da, an observation made previously (40). We advance that there is a retroaldol elimination of the ligand's C₆ hydroxyethyl substituent (see Figure 5 and discussion below).

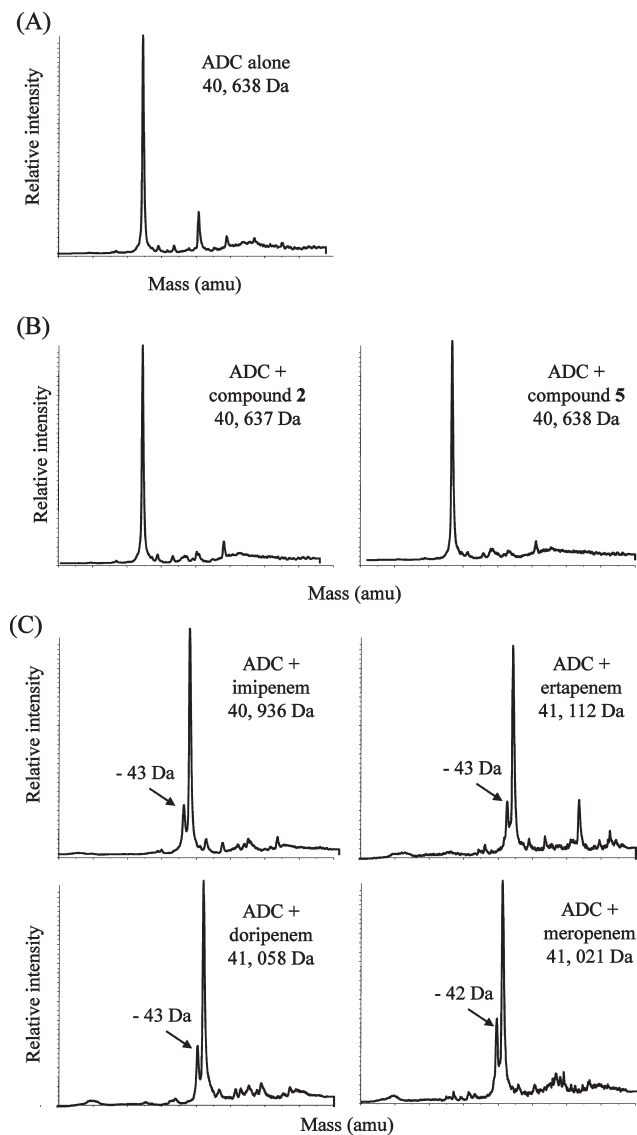


FIGURE 4: Deconvoluted mass spectra of (A) ADC β -lactamase alone, (B) ADC after incubation with compounds **2** and **5** for 15 min, and (C) ADC β -lactamase after incubation with imipenem, ertapenem, doripenem, and meropenem for 15 min. The peak in each ADC–boronate spectrum corresponds to the unmodified ADC enzyme. The major peak in each of the ADC–carbapenem spectra indicates covalent attachment of the β -lactam with a minor additional peak corresponding to the acyl–enzyme intermediate without the carbapenem's C₆ hydroxyethyl substituent. All measurements have an error of ± 3 atomic mass units (amu).

Susceptibility Testing. Nanomolar affinity inhibitors are clinically useful only if they can penetrate the outer cell wall of Gram-negative organisms and restore susceptibility to partner β -lactams. To this end, we performed MIC testing using compounds **3** and **5**. Our results show that when ADC β -lactamase is expressed in the uniform *E. coli* DH10B background, the cephalothin analogues **3** and **5** lower MICs to ceftazidime and cefotaxime (from 16 to 8 and 4 $\mu\text{g}/\text{mL}$ and from 8 to 2 and 1 $\mu\text{g}/\text{mL}$, respectively) (Table 3).

Our previous data showed that *E. coli* DH10B harboring *bla*_{ADC} have MICs of 0.06 $\mu\text{g}/\text{mL}$ with respect to meropenem, ertapenem, and imipenem–cilistatin (26). Thus, we did not perform MIC testing with the carbapenems in combination with the cephalothin analogues as a reduction in susceptibility would be difficult to detect.

Molecular Representations. To understand the interactions between the carbapenems and high-affinity cephalothin analogue **5** in the absence of a crystal structure, we constructed a molecular model of ADC β -lactamase from a homology modeling server. Accurate high-resolution protein models can be generated from templates with $> 50\%$ sequence similarity; our model shared 66% sequence similarity with the template (41).

We first compared our ADC model to the defined crystal structures of *En. cloacae* P99 and *E. coli* AmpC. An alignment based on the predicted, and known, secondary structures of ADC, P99, and *E. coli* AmpC shows that ADC shares 63% sequence similarity with both the P99 and *E. coli* AmpC β -lactamases (37 and 40% amino acid identity, respectively) (Figure 4 of the Supporting Information).

Using the representation of the ADC–**5** acyl–enzyme, we gained insight into how the *Acinetobacter* cephalosporinase interacts with compound **5**. As the crystal structure of the *E. coli* AmpC in complex with the same boronic acid derivative has been determined ($K_i = 1$ nM; PDB entry 1MXO), we overlaid this structure on our generated model (Figure 6) (15). The overall tertiary structures of ADC and the *E. coli* AmpC are similar with conservation of the α -helix and β -sheet domains. The loops and turns between these secondary structures follow slightly different paths, but we note that these deviations may be part of the model construction and are allowable (e.g., the permission of increased flexibility for these strand regions).

In the active site, the backbone amides of Ser64 and Ser318, which form the β -lactamase oxyanion hole or electrophilic center, are ~ 1 Å farther apart in the ADC model than in the *E. coli* AmpC structure (42, 43). The position of the backbones and side chains of the catalytically important Tyr150 and Lys67 also varies by approximately 2 Å between the enzymes (44, 45). Thus, our model suggests that ADC may harbor a unique binding region as compared to the *E. coli* AmpC. These tertiary features are reflected in the disposition of compound **5** in the ADC acyl–enzyme model; in Figure 7, we show that the inhibitor may adopt different conformations in these class C β -lactamases. Comparing equivalent atoms of the boronic acid derivatives (e.g., the *meta*-carboxylate carbons or thiophene sulfur atoms) reveals a > 5 Å deviation in the configuration of the compounds in the overlaid structures. Crystal structures of boronic acid derivatives with AmpC enzymes typically show that one boronic acid oxygen atom is placed in the oxyanion hole formed by residues 64 and 318, and the other oxygen atom forms a hydrogen bond with Tyr150 (15, 17, 44, 46). In the ADC–**5** model, one of the boronic acid hydroxyl groups interacts with the Ser64 backbone carbonyl oxygen, but as the boronic acid and chiral substituents on the inhibitor are rotated approximately 120° compared to those of the *E. coli* β -lactamase structure, both oxygens are approximately 5 Å from Ser318 or Tyr150. Instead, Tyr150 is within ~ 3 Å of both the carbonyl oxygen and thiophene ring sulfur atom from the cephalothin R₁ group of the boronic acid derivative. Our model also shows a hydrogen bond between this R₁ carbonyl oxygen and Lys67. Thus, the residues contributing to the high affinity of this inhibitor for these two β -lactamases may play different roles in each AmpC.

In our kinetic studies, we noted 15-fold differences between the K_i values of the highest-affinity carbapenem (imipenem) and the lowest-affinity carbapenem (meropenem). As these compounds differ primarily in their R₂ side chains, we created models of the ADC–imipenem and ADC–meropenem acyl–enzyme

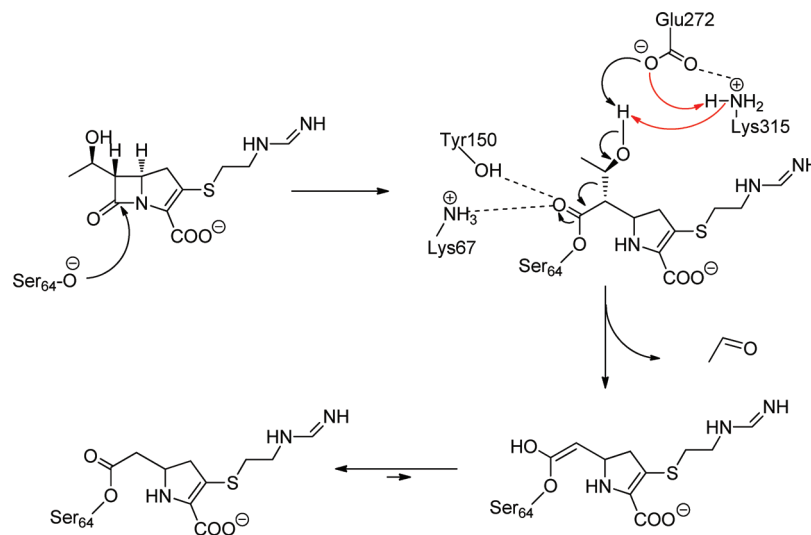


FIGURE 5: Proposed mechanism of the retroaldolic reaction leading to elimination of the C₆ hydroxyethyl substituent from the β -lactamase-carbapenem acyl-enzyme intermediate. Glu272, supported by Lys315, may serve as the base to deprotonate the alcoholic function β -hydroxy carbonyl moiety of the C₆ substituent. Alternatively, Glu272 may abstract a proton from Lys315 which subsequently deprotonates the C₆ group (mechanism colored red). The incipient negative charge on the β -lactam carbonyl could be supported by Tyr150 and Lys67.

Table 3: MIC Values (micrograms per milliliter) of Ceftazidime and Cefotaxime in Combination with 4 μ g/mL Cephalothin Analogues

	<i>E. coli</i> DH10B	<i>E. coli</i> DH10B <i>bla</i> _{ADC}
ceftazidime	1	16
ceftazidime-compound 3	1	8
ceftazidime-compound 5	1	4
cefotaxime	0.06	8
cefotaxime-compound 3	0.06	2
cefotaxime-compound 5	0.06	1

intermediates to explore the K_i contributions of these substituents (Figure 8A,B). On the basis of the MS results indicating the presence of species corresponding to the acyl-enzyme intermediate both with and without the C₆ hydroxyethyl group of the carbapenems, we constructed representations of intact imipenem and meropenem as well as these compounds without their C₆ hydroxyethyl group. Our models predict that when the hydroxyethyl group is present, the carbonyl oxygen from the β -lactam ring of both imipenem and meropenem is located outside of the enzyme's electrophilic, or oxyanion, hole created by the backbone nitrogen atoms of Ser64 and Ser318 (47, 48). Rather, the imipenem β -lactam carbonyl is hydrogen bonded to Lys67, and the meropenem β -lactam carbonyl is only 1.5 Å from Tyr150. The R₂ side chain for both intact carbapenems is oriented out of the active site in the acyl-enzyme intermediate.

In contrast, when the C₆ hydroxyethyl group is removed, the conformation of the carbapenem is significantly changed. Most notably, the β -lactam carbonyl rotates toward the oxyanion hole, approximately 90° in imipenem, and entirely into the electrophilic pocket for meropenem. Further, the R₂ side chain of imipenem flips back toward the active site so that the terminal amide group is ~11 Å from its position in the complex with the C₆ group. The imipenem R₂ group now interacts with Tyr150, Asn152, Lys67, and Gln120. Modeling without the hydroxyethyl group for meropenem changes the conformation of the R₂ group, but it remains oriented outside of the binding site. For both imipenem and meropenem, the model without the C₆ hydroxyethyl group is more energetically favorable, as calculated by the final potential energy of the complexes ($\Delta - 520$ and $\Delta - 80$ kcal/mol, respectively).

DISCUSSION

Our analysis shows that high-affinity inhibition of the ADC β -lactamase, a class C cephalosporinase of increasing medical importance, is a realistic goal. We assayed two types of inhibitors against ADC: (i) compounds that resemble the natural substrate for the *Acinetobacter* cephalosporinase and (ii) the currently available carbapenems. This approach teaches us important lessons about the inhibition of this clinically challenging β -lactamase and elucidates contributions of R₁ and R₂ side chains. We begin with an examination of the data revealing the low micromolar K_i values of the ADC β -lactamase by the carbapenems and then discuss how the boronic acid derivatives, as chemical probes, yield important insights into the nature of class C enzyme active sites.

After incubation of ADC and each carbapenem, our ESI-MS data reveal the formation of two molecular species. The mass of the predominant species corresponds to the intact carbapenem acylating ADC; the mass of the minor species corresponds to that of the acyl-enzyme intermediate minus 43 Da (Table 2). On the basis of previous MS studies in our and other laboratories, we assign the major peak to the carbapenem acyl-enzyme species (21, 40). Formation of a stable acyl-enzyme intermediate is supported by previously defined crystal structures of carbapenems and class A and C β -lactamases (18, 20, 21). Our ADC-imipenem and ADC-meropenem acyl-enzyme models show conformations in which the β -lactam carbonyl oxygen is not found in the oxyanion hole formed by the backbone nitrogens of residues Ser64 and Ser318. This observation is consistent with the X-ray crystal structure of the *E. coli* AmpC β -lactamase with imipenem where the carbonyl was positioned approximately 180° outside of the oxyanion hole (18). Additional crystal structures of class A β -lactamases in complex with carbapenems have also shown this repositioning of the β -lactam carbonyl (20, 21). This displacement is likely precipitated by steric interactions induced by the carbapenems' C₆ hydroxyethyl groups, producing a conformational change that forces the carbonyl away from the oxyanion hole and into a position unfavorable for hydrolysis (20, 42, 43). This reasoning offers an explanation for the inhibition of the *Acinetobacter* cephalosporinase by the carbapenems.

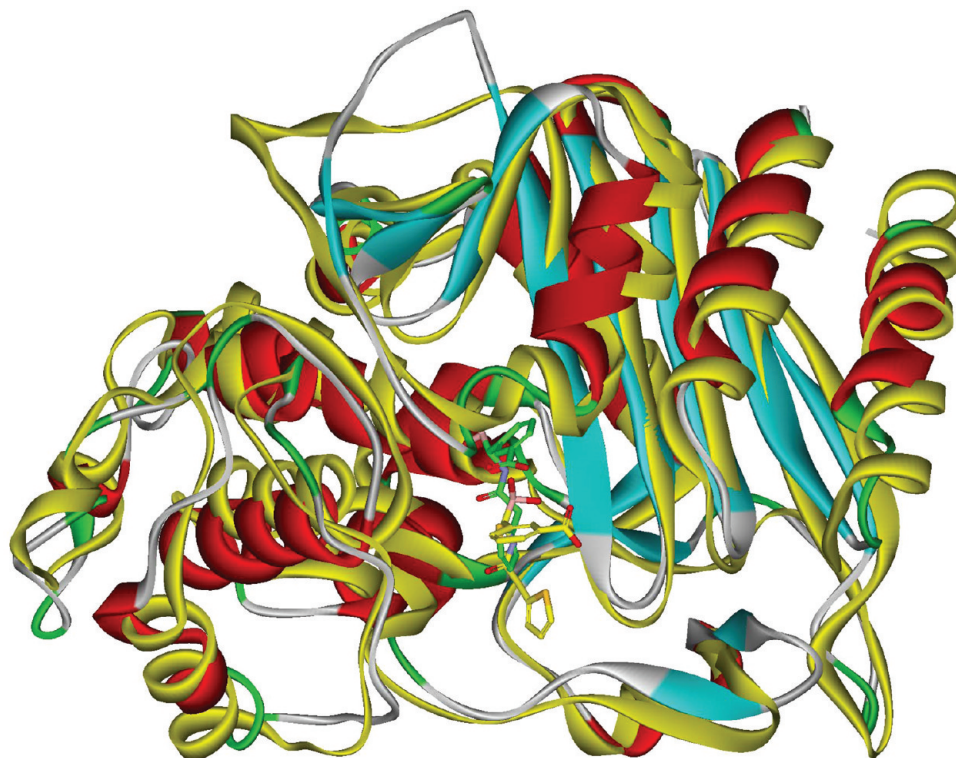


FIGURE 6: Overlay of molecular coordinates for the *E. coli* AmpC–5 complex colored yellow (PDB entry 1MXO) and generated ADC–5 model colored by secondary structure. The position of α -helices and β -sheets is generally preserved between the two proteins, but deviations are observed in the strand turns between these secondary structures. Active site differences are illustrated by the altered conformation of 5 (colored green) in ADC as compared to 5 (colored yellow) bound to the *E. coli* AmpC.

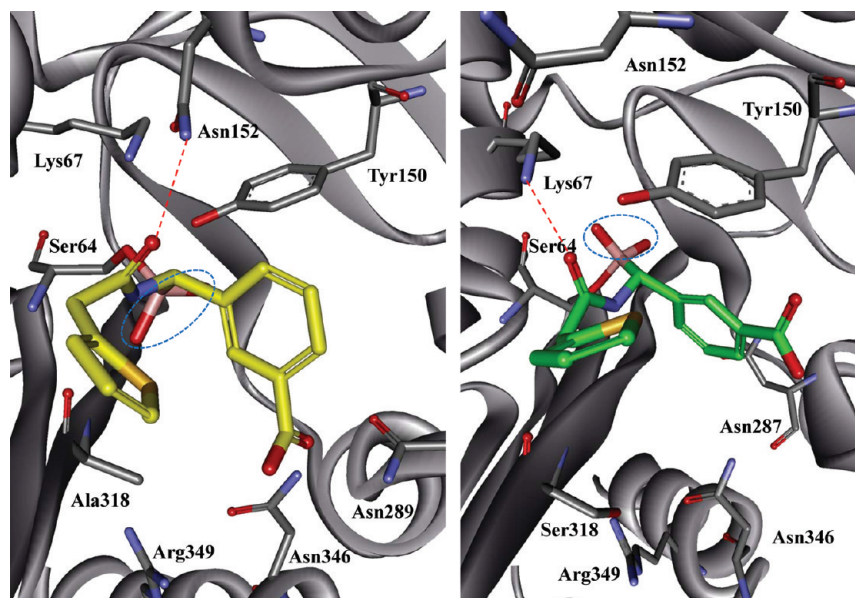


FIGURE 7: Comparison of the binding site interactions between the *E. coli* AmpC–5 (left) and ADC–5 (right) models. Figures have a perspective view to show positions of the residues in relation to the inhibitor. The boronic acid derivative is bound to Ser64 in both structures, but the relative rotation of the inhibitor in ADC changes the relationships with other active site residues. Specifically, the boronic acid oxygens (circled in dashed blue lines) interact with Ala318 and Tyr150 in *E. coli* AmpC, but the hydrogen bond with Ser318 is lost in ADC. Also in ADC, the *meta*-carboxylate of the dihydrothiazine ring analogue has no clear interaction with previously identified carboxylate binding residues (e.g., Asn346, Arg349, or Asn289 in *E. coli* AmpC). Instead, the group may form a long hydrogen bond with Asn287. The carbonyl oxygen of the cephalothin R₁ side chain interacts with Asn152 in *E. coli* AmpC but is reoriented toward Lys67 in ADC (see dashed red lines). Lastly, the R₁ thiophene ring sulfur in the ADC–5 model is moved toward Tyr150 as compared to the *E. coli* AmpC–5 structure. Overall, these significant active site differences suggest that while ADC may possess novel architecture, the ability to recognize inhibitors and substrates is preserved because of the versatile functions of the binding site residues.

Second, we observed a minor peak in each ADC–carbapenem spectrum that reflects the elimination of the carbapenem C₆ hydroxyethyl group. This observation was reported previously in

the class A *Mycobacterium tuberculosis* blaC (40). Our molecular representations of imipenem and meropenem in complex with ADC give us insights into how the carbapenems are behaving in

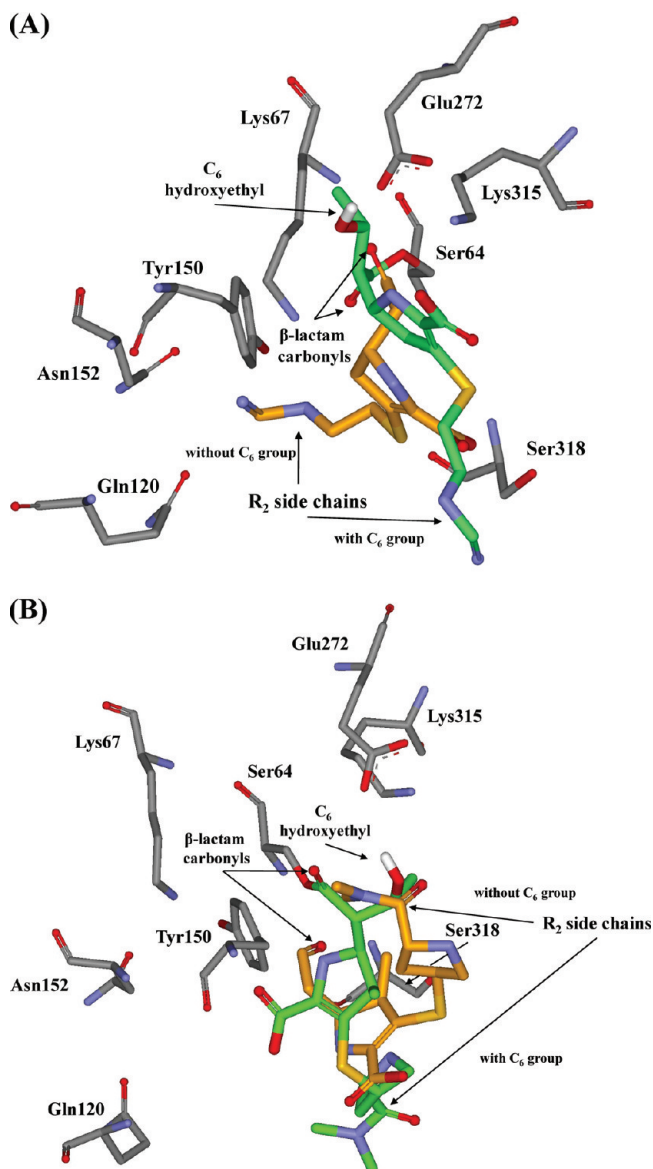


FIGURE 8: Molecular representation of (A) the ADC–imipenem acyl–enzyme model and (B) the ADC–meropenem acyl–enzyme model. The intact carbapenem is colored green and the carbapenem without the C_6 hydroxyethyl group orange. Hydrogens are not shown except on the carbapenem C_6 hydroxyethyl which is likely deprotonated by Glu272, leading to elimination of the group. Removal of this C_6 substituent may lead to reorientation of the compound in the active site. Specifically, the β -lactam carbonyl moves back toward the oxyanion hole formed by the backbone nitrogens of Ser64 and Ser318, an approximately 90° rotation for imipenem and entirely into the hole for meropenem. Also after C_6 elimination, the R_2 group of imipenem is repositioned from outside of the binding pocket into a network of interactions with Tyr150, Asn152, Lys67, and Gln120. Active site interactions are not observed for the R_2 group of meropenem, which may have implications for the differing K_i values of these carbapenems.

the active site of ADC following this elimination. When the C_6 hydroxyethyl group is removed from the carbapenem, both compounds adopt new positions in which the β -lactam carbonyl moves to be either entirely in the oxyanion hole (meropenem) or rotated back toward the hole approximately 90° (imipenem). This prediction is similar to the conclusion drawn from the X-ray crystallographic evidence of the class A Asn132Ala TEM enzyme variant which demonstrated that the substitution allowed the β -lactam carbonyl to rotate back into the oxyanion hole (49). We

speculate that removal of the C_6 group is an alternative mechanism of alleviating the steric clashes induced by this substituent, allowing repositioning of the acyl–enzyme intermediate. When the β -lactam carbonyl is aligned in the oxyanion hole, the conformation is more compatible with hydrolysis, and an increased level of turnover is likely, consistent with the relatively small amount of this species evident on ESI-MS. Furthermore, we observe this process after a 15 min incubation, which is within the bacterial generation time (i.e., 20 min) and suggests that this elimination may be occurring in cells.

The mechanism of elimination of the hydroxyethyl group is likely to be a retroaldolic-type reaction of the β -hydroxyethyl moiety of the β -lactamase acyl–enzyme intermediate (Figure 5). We propose that Glu272, supported by Lys315, may serve as the base to deprotonate directly the alcoholic function of the C_6 substituent. Alternatively, Glu272 may abstract a proton from the amine side chain of Lys315, and then Lys315 would then deprotonate the carbapenem C_6 alcohol group. In either case, the negative charge on the β -lactam carbonyl could be stabilized by Tyr150 and Lys67. Interestingly, this proposes another role for Tyr150, which is already implicated in both acylation and “substrate-activated catalysis” in AmpC enzymes (44, 45, 50, 51). This mechanism is consistent with our molecular representations which show Glu272 within hydrogen bonding distance of the C_6 hydroxyethyl group for both imipenem and meropenem; the Lys315, Tyr150, and Lys67 residues are also positioned to support this reaction (see Figure 8A,B). Further investigation of these residues and their potential roles in the retroaldolic-type reaction will help elucidate the C_6 elimination mechanism.

Structural and kinetic studies provide evidence that, following acylation of carbapenems by β -lactamases, the acyl–enzyme intermediate formed can tautomerize between a Δ^2 - and Δ^1 -pyrroline species that have differing rates of deacylation (19, 52–55). We modeled both the tautomers in our molecular representations with ADC, but the interactions between the enzyme and the carbapenems were not significantly different for either the Δ^1 or Δ^2 species. We anticipate that the Δ^2 – Δ^1 tautomerization exists as both a separate and integrated pathway to C_6 hydroxyethyl group elimination and plan further examination of the reaction and its implications for inhibition.

We next turn our attention to the contribution of the R_2 side chain to the differing K_i values of the carbapenems for the ADC β -lactamase. The four carbapenems tested share a common β -lactam ring scaffold and vary by their R_2 substituents, yet we observed up to 15-fold differences in K_i values. Our models offer insights into how these side groups interact with the ADC enzyme and suggest that each carbapenem may behave uniquely. In both the imipenem and meropenem models including the C_6 hydroxyethyl group, the R_2 side chain is oriented out of the active site and does not engage in significant interactions with the enzyme. This outward conformation is also seen in the *E. coli* AmpC–imipenem, TEM–imipenem, and SHV–meropenem crystal structures (PDB entries 1LL5, 1BT5, and 2ZD8, respectively) (18, 20, 21). However, upon removal of the C_6 hydroxyethyl group, the R_2 side chain of imipenem rotates toward the binding pocket and interacts with several active site residues, including Tyr150, Asn152, Lys67, and Gln120. In contrast, the R_2 group of meropenem modeled without the C_6 hydroxyethyl group is still positioned away from active site residues. In light of the K_i measurements for these two carbapenems, the molecular representations predict that the interactions between the R_2 group of imipenem and ADC may stabilize this

form of the compound in the active site, while for meropenem, the interactions with the enzyme are less favorable (e.g., electrostatically or sterically). Notably, the R₂ group of imipenem is the least substituted of those of the carbapenems, and the additional atoms and ring structures of meropenem, doripenem, and ertapenem may affect the K_i values by various mechanisms, e.g., limiting conformational flexibility necessary for rotating back toward the active site to make favorable interactions. We note that the R₂ side chain of imipenem in the crystal structure with TEM Asn132Ala remains oriented out of the active site, despite the alleviation of the steric strain caused by the C₆ substituent (PDB entry 1JVJ) (49). That our model of imipenem without the C₆ hydroxyethyl group leads to significant R₂ conformational change may reflect inherent differences between the inhibition of class A and C β-lactamases by carbapenems, perhaps partly due to the increased size of the active site in class C enzymes (56).

We now highlight the versatile β-lactamase inhibitory activity of the rationally designed boronic acid derivatives (13, 14). All the cephalosporin analogues had K_i values of ≤1 μM, and these values likely reflect the naturally high affinity of AmpC enzymes for cephalosporin substrates (24). Interestingly, compounds 1–3 which contain only the cephalosporin R₁ side chains have very similar K_i values, suggesting limited differences in the affinity gains of these R₁ structures. The kinetic substrate profile of ADC, and AmpCs in general, includes increasing affinities for the larger side chains of “third-generation” cephalosporins, which would include ceftazidime and cefoperazone (24, 26, 57). “First-generation” cephalosporins, such as cephalothin, typically have lower affinities but higher hydrolytic rates. Thus, despite these differences in affinity and hydrolytic rates, the first- and third-generation cephalosporin analogues have comparable K_i values as inhibitors.

The introduction of chirality and the substituent resembling the dihydrothiazine ring of the cephalosporin nucleus leads to a 22-fold increase in affinity (compound 3 vs 4). The further addition of the C₄ carboxylate leads to a 70-fold increase over that of the achiral counterpart (compound 3 vs 5). Compound 5, which incorporates these multiple structural features of the cephalosporins, displays the lowest K_i for the ADC enzyme. Our results indicating the contribution of the *meta*-carboxyphenyl ring on the K_i of compound 5 are consistent with previous data demonstrating the importance of this functional group for molecular recognition in class C AmpC β-lactamases (15, 31). The crystal structure of compound 5 in complex with the *E. coli* AmpC β-lactamase shows a hydrogen bond between the carboxylate of the inhibitor and the amide of Asn289 (15). This interaction is well-studied, and thermodynamic cycle experiments revealed that the hydrogen bond contributes 1.7 kcal/mol to the overall binding affinity, a value within the range for ion–dipole interaction (58). However, Asn289 is not a well-conserved residue among class C β-lactamases. The K_i of this cephalothin analogue increases from 1 nM with *E. coli* AmpC to 29 nM with *En. cloacae* P99 AmpC which has Ser289, suggesting that the amino acid at position 289 plays a role in the affinity of compound 5 (47, 58).

On the basis of amino acid sequence, the *Acinetobacter* ADC cephalosporinase is not closely related to other AmpCs and has a Glu residue at position 289 (Figure 4 of the Supporting Information). Glu is not a hydrogen bond donor, and our model shows the Glu289 side chain is well outside hydrogen bond distance (~7 Å). Thus, we used our molecular representation of

the ADC–5 complex to search for other residues that could be hydrogen bonding with the *meta*-carboxylate. Previous structural and functional studies of AmpC enzymes suggest that the more conserved sites Xaa343, Asn346, Arg349, and Thr316 interact with the C₃/C₄ carboxylate of the substrate, although none of these residues were involved with the *meta*-carboxylate in the *E. coli*–5 crystal complex (15, 18, 46–48, 59–61). Similarly, each of these residues is at least 5 Å from the *meta*-carboxylate in our ADC–5 representation, an unlikely distance for a high-energy hydrogen bond with the group. Asn287 is an “ancillary” ADC residue which may be capable of engaging the *meta*-carboxylate in a hydrogen bond with ion–dipole character but is positioned approximately 8 Å away in our model (Figure 7). The molecular explanations of the ADC inhibition by the cephalothin analogues 4 and 5 remain to be validated by further study with boronic acid derivatives as molecular probes, site-directed mutagenesis of ADC, and/or crystallography.

AmpC enzyme binding site “hot spots” were previously identified by a comparison of crystal structures in complex with both boronic acid inhibitors and β-lactam substrates (46). Our ADC acyl–enzyme representation reveals that the recognition elements may differ for the ADC β-lactamase. For example, the *E. coli* AmpC hydroxyl binding site was defined by Tyr150 and its hydrogen bond with one of the boronic acid hydroxyls, displacing the deacylation water (15, 44). Our ADC–5 model shows significant repositioning of the boronic acid group, making this interaction with Tyr150 unlikely. Rather, the ADC Tyr150 is within ~3 Å of the thiophene sulfur and carbonyl oxygen found in the R₁ side chain of compound 5. Further, the R₁ amide recognition site formed by the interaction of the R₁ carbonyl and Asn152 in the *E. coli* AmpC differs from our ADC–5 representation, as this same side chain carbonyl forms a hydrogen bond with Lys67 (46). These consensus binding sites were compiled exclusively from crystal structures of *E. coli* AmpC, and our kinetic data and modeling analyses indicate the ADC β-lactamase may interact differently with boronic acid inhibitors versus other class C enzymes (15, 46, 58). Our molecular representations of ADC in complex with the inhibitors were useful for developing hypotheses; however, we remain cognizant of modeling limitations, such as the lack of active site flexibility and the removal of water molecules during the ligand docking protocol.

That the chiral cephalothin analogue 5 can maintain a low nanomolar K_i for several phylogenetically divergent AmpC β-lactamases reflects not only the potency of this inhibitor but also what may be an important plasticity of AmpCs (26, 46, 58). The significant repositioning of the boronic acid derivative revealed in our ADC–5 model may be an indication of this enzyme’s versatility, causing the β-lactamase–ligand interactions to have different molecular correlates. We posit that compounds 4 and 5 benefit from the presence of an additional side chain which more closely resembles the dihydrothiazine ring of the natural substrate, cephalosporins. The stereochemistry and conformation of the chiral inhibitors may create a better “fit” for this enzyme. In part, this improved fit may be due to approximation of the deacylation transition state of the cephalosporinase, a theory which has been previously offered to explain the high affinity of chiral boronic acid derivatives (33, 44).

Hence, the notion of dedicated AmpC enzyme R₁ and R₂ binding sites may be especially fluid and adaptable in ADC, permitting the β-lactamase to change recognition elements depending on the ligand (46, 56). These novel interactions may reflect the fact that differences in primary sequence can be

compensated by common secondary and tertiary structures, allowing the enzyme to use multiple ancillary residues to make contact with substrates and inhibitors. Alternatively, ADC may have subtle differences in its deacylation mechanism which is suggested by the unanticipated position of the boronic acid oxygen atoms in our model. This AmpC structure–function redundancy merits further study, as it could both lie at the core of why these β -lactamases have evolved as versatile “traps” of cephalosporin substrates but also aid the careful design of broad-spectrum inhibitors (62, 63).

Despite the description of boronates as β -lactamase inhibitors since the 1970s, boronic acid derivatives have not yet been developed for clinical use in combination with a β -lactam (64). Concerns about the safety and efficacy of boron-containing therapeutics are currently being addressed by clinical studies sponsored by the pharmaceutical industry (65). The data presented in this paper encourage the *in vivo* study of boronates as β -lactamase inhibitors.

CONCLUSION

In summary, we provide important insights into the interaction of two types of inhibitors with the *Acinetobacter* and other clinically relevant cephalosporinases. First, we present kinetic data and molecular representations that explain why carbapenems are effective inhibitors of class C enzymes, including formation of a stable acyl–enzyme intermediate and a role for the compounds' R₂ side groups. Our results add to a growing body of evidence supporting the activity of carbapenems as broad-spectrum β -lactam antibiotics, “slow substrates”, and inactivators of class A and C β -lactamases (18–21, 23–25). Second, our ADC model suggests that inhibitors designed to mimic the structure of natural substrates (i.e., boronic acid derivatives) may adopt unique conformations in different class C active sites. Despite significant sequence and structure dissimilarity between ADC and the *E. coli* AmpC, the chiral cephalothin analogues attain similar K_i values for both enzymes. This versatility may reflect an important plasticity of this cephalosporinase β -lactamase. Our data offer promise for the development of compounds that have an extended inhibition profile across, and within, β -lactamase classes, and specifically against this challenging *Acinetobacter* spp. target.

ACKNOWLEDGMENT

We thank Dr. Andrea Endimiani and Ms. Andrea Hujer for careful review of the manuscript.

SUPPORTING INFORMATION AVAILABLE

ADC β -lactamase model validation reports and multiple-sequence protein alignment of crystal structure coordinates for *En. cloacae* P99 (PDB entry 1XX2), *E. coli* AmpC (PDB entry 2BLS), and the ADC model. This material is available free of charge via the Internet at <http://pubs.acs.org>.

REFERENCES

1. Fournier, P. E., and Richet, H. (2006) The epidemiology and control of *Acinetobacter baumannii* in health care facilities. *Clin. Infect. Dis.* 42, 692–699.
2. Poirel, L., Karim, A., Mercat, A., Le Thomas, I., Vahaboglu, H., Richard, C., and Nordmann, P. (1999) Extended-spectrum β -lactamase-producing strain of *Acinetobacter baumannii* isolated from a patient in France. *J. Antimicrob. Chemother.* 43, 157–158.
3. Cisneros, J. M., and Rodriguez-Bano, J. (2002) Nosocomial bacteremia due to *Acinetobacter baumannii*: Epidemiology, clinical features and treatment. *Clin. Microbiol. Infect.* 8, 687–693.
4. Gootz, T. D., and Marra, A. (2008) *Acinetobacter baumannii*: An emerging multidrug-resistant threat. *Expert Rev. Anti-Infect. Ther.* 6, 309–325.
5. Perez, F., Hujer, A. M., Hujer, K. M., Decker, B. K., Rather, P. N., and Bonomo, R. A. (2007) Global challenge of multidrug-resistant *Acinetobacter baumannii*. *Antimicrob. Agents Chemother.* 51, 3471–3484.
6. Vila, J., Marti, S., and Sanchez-Cespedes, J. (2007) Porins, efflux pumps and multidrug resistance in *Acinetobacter baumannii*. *J. Antimicrob. Chemother.* 59, 1210–1215.
7. Livermore, D. M., and Woodford, N. (2006) The β -lactamase threat in *Enterobacteriaceae*, *Pseudomonas*, and *Acinetobacter*. *Trends Microbiol.* 14, 413–420.
8. Bonomo, R. A., and Szabo, D. (2006) Mechanisms of multidrug resistance in *Acinetobacter* species and *Pseudomonas aeruginosa*. *Clin. Infect. Dis.* 43 (Suppl. 2), S49–S56.
9. Peleg, A. Y., Seifert, H., and Paterson, D. L. (2008) *Acinetobacter baumannii*: Emergence of a successful pathogen. *Clin. Microbiol. Rev.* 21, 538–582.
10. Perez, F., Endimiani, A., and Bonomo, R. A. (2008) Why are we afraid of *Acinetobacter baumannii*? *Expert Rev. Anti-Infect. Ther.* 6, 269–271.
11. Bou, G., Cervero, G., Dominguez, M. A., Quereda, C., and Martinez-Beltran, J. (2000) Characterization of a nosocomial outbreak caused by a multiresistant *Acinetobacter baumannii* strain with a carbapenem-hydrolyzing enzyme: High-level carbapenem resistance in *A. baumannii* is not due solely to the presence of β -lactamases. *J. Clin. Microbiol.* 38, 3299–3305.
12. Levin, A. S. (2003) Treatment of *Acinetobacter* spp infections. *Expert Opin. Pharmacother.* 4, 1289–1296.
13. Beesley, T., Gascoyne, N., Knott-Hunziker, V., Petursson, S., Waley, S. G., Jaurin, B., and Grundstrom, T. (1983) The inhibition of class C β -lactamases by boronic acids. *Biochem. J.* 209, 229–233.
14. Crompton, I. E., Cuthbert, B. K., Lowe, G., and Waley, S. G. (1988) β -Lactamase inhibitors. The inhibition of serine β -lactamases by specific boronic acids. *Biochem. J.* 251, 453–459.
15. Morandi, F., Caselli, E., Morandi, S., Focia, P. J., Blazquez, J., Shoichet, B. K., and Prati, F. (2003) Nanomolar inhibitors of AmpC β -lactamase. *J. Am. Chem. Soc.* 125, 685–695.
16. Weston, G. S., Blazquez, J., Baquero, F., and Shoichet, B. K. (1998) Structure-based enhancement of boronic acid-based inhibitors of AmpC β -lactamase. *J. Med. Chem.* 41, 4577–4586.
17. Caselli, E., Powers, R. A., Blaszczak, L. C., Wu, C. Y., Prati, F., and Shoichet, B. K. (2001) Energetic, structural, and antimicrobial analyses of β -lactam side chain recognition by β -lactamases. *Chem. Biol.* 8, 17–31.
18. Beadle, B. M., and Shoichet, B. K. (2002) Structural basis for imipenem inhibition of class C β -lactamases. *Antimicrob. Agents Chemother.* 46, 3978–3980.
19. Taibi, P., and Mobashery, S. (1995) Mechanism of turnover of imipenem by the TEM β -lactamase revisited. *J. Am. Chem. Soc.* 117, 7600–7605.
20. Maveyraud, L., Mourey, L., Kotra, L. P., Pedelacq, J.-D., Guillet, V., and Mobashery, S. (1998) Structural basis for clinical longevity of carbapenem antibiotics in the face of challenge by the common class A β -lactamases from the antibiotic-resistant bacteria. *J. Am. Chem. Soc.* 120, 9748–9752.
21. Nukaga, M., Bethel, C. R., Thomson, J. M., Hujer, A. M., Distler, A., Anderson, V. E., Knox, J. R., and Bonomo, R. A. (2008) Inhibition of class A β -lactamases by carbapenems: Crystallographic observation of two conformations of meropenem in SHV-1. *J. Am. Chem. Soc.* 130, 12656–12662.
22. Pernot, L., Frenois, F., Rybkine, T., L'Hermite, G., Petrella, S., Delettre, J., Jarlier, V., Collatz, E., and Sougakoff, W. (2001) Crystal structures of the class D β -lactamase OXA-13 in the native form and in complex with meropenem. *J. Mol. Biol.* 310, 859–874.
23. Monks, J., and Waley, S. G. (1988) Imipenem as substrate and inhibitor of β -lactamases. *Biochem. J.* 253, 323–328.
24. Galleni, M., Amicosante, G., and Frere, J. M. (1988) A survey of the kinetic parameters of class C β -lactamases. Cephalosporins and other β -lactam compounds. *Biochem. J.* 255, 123–129.
25. Matagne, A., Ghuyssen, M. F., and Frere, J. M. (1993) Interactions between active-site-serine β -lactamases and mechanism-based inactivators: A kinetic study and an overview. *Biochem. J.* 295 (Part 3), 705–711.
26. Hujer, K. M., Hamza, N. S., Hujer, A. M., Perez, F., Helfand, M. S., Bethel, C. R., Thomson, J. M., Anderson, V. E., Barlow, M., Rice,

- L. B., Tenover, F. C., and Bonomo, R. A. (2005) Identification of a new allelic variant of the *Acinetobacter baumannii* cephalosporinase, ADC-7 β -lactamase: Defining a unique family of class C enzymes. *Antimicrob. Agents Chemother.* 49, 2941–2948.
27. Thomson, J. M., Distler, A. M., Prati, F., and Bonomo, R. A. (2006) Probing active site chemistry in SHV β -lactamase variants at Ambler position 244. Understanding unique properties of inhibitor resistance. *J. Biol. Chem.* 281, 26734–26744.
28. Hujer, A. M., Hujer, K. M., Helfand, M. S., Anderson, V. E., and Bonomo, R. A. (2002) Amino acid substitutions at Ambler position Gly238 in the SHV-1 β -lactamase: Exploring sequence requirements for resistance to penicillins and cephalosporins. *Antimicrob. Agents Chemother.* 46, 3971–3977.
29. Pattanaik, P., Bethel, C. R., Hujer, A. M., Hujer, K. M., Distler, A. M., Taracila, M., Anderson, V. E., Fritsche, T. R., Jones, R. N., Pagadala, S. R., van den Akker, F., Buynak, J. D., and Bonomo, R. A. (2009) Strategic Design of an Effective β -Lactamase Inhibitor: LN-1–255, a 6-alkylidene-2'-substituted penicillin sulfone. *J. Biol. Chem.* 284, 945–953.
30. De Meester, F., Joris, B., Reckinger, G., Bellefroid-Bourguignon, C., Frere, J. M., and Waley, S. G. (1987) Automated analysis of enzyme inactivation phenomena. Application to β -lactamases and DD-peptidases. *Biochem. Pharmacol.* 36, 2393–2403.
31. Morandi, S., Morandi, F., Caselli, E., Shoichet, B. K., and Prati, F. (2008) Structure-based optimization of cephalothin-analogue boronic acids as β -lactamase inhibitors. *Bioorg. Med. Chem.* 16, 1195–1205.
32. Chen, Y., Shoichet, B., and Bonnet, R. (2005) Structure, function, and inhibition along the reaction coordinate of CTX-M β -lactamases. *J. Am. Chem. Soc.* 127, 5423–5434.
33. Wang, X., Minasov, G., Blazquez, J., Caselli, E., Prati, F., and Shoichet, B. K. (2003) Recognition and resistance in TEM β -lactamase. *Biochemistry* 42, 8434–8444.
34. Arnold, K., Bordoli, L., Kopp, J., and Schwede, T. (2006) The SWISS-MODEL workspace: A web-based environment for protein structure homology modelling. *Bioinformatics* 22, 195–201.
35. Kim, J. Y., Jung, H. I., An, Y. J., Lee, J. H., Kim, S. J., Jeong, S. H., Lee, K. J., Suh, P. G., Lee, H. S., Lee, S. H., and Cha, S. S. (2006) Structural basis for the extended substrate spectrum of CMY-10, a plasmid-encoded class C β -lactamase. *Mol. Microbiol.* 60, 907–916.
36. Melo, F., and Feytmans, E. (1998) Assessing protein structures with a non-local atomic interaction energy. *J. Mol. Biol.* 277, 1141–1152.
37. Laskowski, R. A., MacArthur, M. W., Moss, D., and Thornton, J. M. (1993) PROCHECK: A program to check the stereochemical quality of protein structures. *J. Appl. Crystallogr.* 26, 283–291.
38. Thompson, J. D., Higgins, D. G., and Gibson, T. J. (1994) CLUSTAL W: Improving the sensitivity of progressive multiple sequence alignment through sequence weighting, position-specific gap penalties and weight matrix choice. *Nucleic Acids Res.* 22, 4673–4680.
39. Diller, D. J., and Merz, K. M., Jr. (2001) High throughput docking for library design and library prioritization. *Proteins* 43, 113–124.
40. Hugonnet, J. E., Tremblay, L. W., Boshoff, H. I., Barry, C. E. III, and Blanchard, J. S. (2009) Meropenem-clavulanate is effective against extensively drug-resistant *Mycobacterium tuberculosis*. *Science* 323, 1215–1218.
41. Kryshchuk, A., and Fidelis, K. (2009) Protein structure prediction and model quality assessment. *Drug Discovery Today* 14, 386–393.
42. Murphy, B. P., and Pratt, R. F. (1988) Evidence for an oxyanion hole in serine β -lactamases and DD-peptidases. *Biochem. J.* 256, 669–672.
43. Usher, K. C., Blaszczak, L. C., Weston, G. S., Shoichet, B. K., and Remington, S. J. (1998) Three-dimensional structure of AmpC β -lactamase from *Escherichia coli* bound to a transition-state analogue: Possible implications for the oxyanion hypothesis and for inhibitor design. *Biochemistry* 37, 16082–16092.
44. Chen, Y., Minasov, G., Roth, T. A., Prati, F., and Shoichet, B. K. (2006) The deacylation mechanism of AmpC β -lactamase at ultrahigh resolution. *J. Am. Chem. Soc.* 128, 2970–2976.
45. Gherman, B. F., Goldberg, S. D., Cornish, V. W., and Friesner, R. A. (2004) Mixed quantum mechanical/molecular mechanical (QM/MM) study of the deacylation reaction in a penicillin binding protein (PBP) versus in a class C β -lactamase. *J. Am. Chem. Soc.* 126, 7652–7664.
46. Powers, R. A., and Shoichet, B. K. (2002) Structure-based approach for binding site identification on AmpC β -lactamase. *J. Med. Chem.* 45, 3222–3234.
47. Lobkovsky, E., Billings, E. M., Moews, P. C., Rahil, J., Pratt, R. F., and Knox, J. R. (1994) Crystallographic structure of a phosphonate derivative of the *Enterobacter cloacae* P99 cephalosporinase: Mechanistic interpretation of a β -lactamase transition-state analog. *Biochemistry* 33, 6762–6772.
48. Zhang, Z., Yu, Y., Musser, J. M., and Palzkill, T. (2001) Amino acid sequence determinants of extended spectrum cephalosporin hydrolysis by the class C P99 β -lactamase. *J. Biol. Chem.* 276, 46568–46574.
49. Wang, X., Minasov, G., and Shoichet, B. K. (2002) Noncovalent interaction energies in covalent complexes: TEM-1 β -lactamase and β -lactams. *Proteins* 47, 86–96.
50. Buluychev, A., Massova, I., Miyashita, K., and Mobashery, S. (1997) Nuances of mechanisms and their implications for evolution of the versatile β -lactamase activity: From biosynthetic enzymes to drug resistance factors. *J. Am. Chem. Soc.* 119, 7619–7625.
51. Oefner, C., D'Arcy, A., Daly, J. J., Gubernator, K., Charnas, R. L., Heinze, I., Hubschwerlen, C., and Winkler, F. K. (1990) Refined crystal structure of β -lactamase from *Citrobacter freundii* indicates a mechanism for β -lactam hydrolysis. *Nature* 343, 284–288.
52. Kalp, M., and Carey, P. R. (2008) Carbapenems and SHV-1 β -lactamase form different acyl-enzyme populations in crystals and solution. *Biochemistry* 47, 11830–11837.
53. Charnas, R. L., and Knowles, J. R. (1981) Inhibition of the RTEM β -lactamase from *Escherichia coli*. Interaction of enzyme with derivatives of olivanic acid. *Biochemistry* 20, 2732–2737.
54. Easton, C. J., and Knowles, J. R. (1982) Inhibition of the RTEM β -lactamase from *Escherichia coli*. Interaction of the enzyme with derivatives of olivanic acid. *Biochemistry* 21, 2857–2862.
55. Zafaralla, G., and Mobashery, S. (1992) Facilitation of the Δ^2 to Δ^1 pyrroline tautomerization of carbapenem antibiotics by the highly conserved arginine-244 of class A β -lactamases during the course of turnover. *J. Am. Chem. Soc.* 114, 1505–1506.
56. Jacoby, G. A. (2009) AmpC β -lactamases. *Clin. Microbiol. Rev.* 22, 161–182.
57. Page, M. G. (1993) The kinetics of non-stoichiometric bursts of β -lactam hydrolysis catalysed by class C β -lactamases. *Biochem. J.* 295 (Part 1), 295–304.
58. Roth, T. A., Minasov, G., Morandi, S., Prati, F., and Shoichet, B. K. (2003) Thermodynamic cycle analysis and inhibitor design against β -lactamase. *Biochemistry* 42, 14483–14491.
59. Dubus, A., Wilkin, J. M., Raquet, X., Normark, S., and Frere, J. M. (1994) Catalytic mechanism of active-site serine β -lactamases: Role of the conserved hydroxy group of the Lys-Thr(Ser)-Gly triad. *Biochem. J.* 301 (Part 2), 485–494.
60. Patera, A., Blaszczak, L. C., and Shoichet, B. (2000) Crystal structures of substrate and inhibitor complexes with AmpC β -lactamase: Possible implications for substrate-assisted catalysis. *J. Am. Chem. Soc.* 122, 10504–10512.
61. Beadle, B. M., Trehan, I., Focia, P. J., and Shoichet, B. K. (2002) Structural milestones in the reaction pathway of an amide hydrolase: Substrate, acyl, and product complexes of cephalothin with AmpC β -lactamase. *Structure* 10, 413–424.
62. Then, R. L., and Angehrn, P. (1982) Trapping of nonhydrolyzable cephalosporins by cephalosporinases in *Enterobacter cloacae* and *Pseudomonas aeruginosa* as a possible resistance mechanism. *Antimicrob. Agents Chemother.* 21, 711–717.
63. Sanders, C. C. (1984) Inducible β -lactamases and non-hydrolytic resistance mechanisms. *J. Antimicrob. Chemother.* 13, 1–3.
64. Kiener, P. A., and Waley, S. G. (1978) Reversible inhibitors of penicillinases. *Biochem. J.* 169, 197–204.
65. Baker, S. J., Akama, T., Zhang, Y. K., Sauro, V., Pandit, C., Singh, R., Kully, M., Khan, J., Plattner, J. J., Benkovic, S. J., Lee, V., and Maples, K. R. (2006) Identification of a novel boron-containing antibacterial agent (AN0128) with anti-inflammatory activity, for the potential treatment of cutaneous diseases. *Bioorg. Med. Chem. Lett.* 16, 5963–5967.